Thermodynamic Anomalies in Stretched Water

Y. Elia Altabet,[†,§] Rakesh S. Singh,[†,§] Frank H. Stillinger,[‡] and Pablo G. Debenedetti*[,†]

[†]Department of Chemical and Biological Engineering, Princeton University, Princeton, New Jersey 08544, United States
[‡]Department of Chemistry, Princeton University, Princeton, New Jersey 08544, United States

ABSTRACT: Via molecular dynamics simulations of the TIP4P/2005 water model, we study liquid water's anomalous behavior at large negative pressure produced through isochoric cooling. We find that isochores without a pressure minimum can display "reentrant" behavior whereby a system that cavitates upon cooling can then rehomogenize upon further cooling. This behavior is a consequence of the underlying density maximum along the spinodal, but its actual manifestation in simulations is strongly influenced by finite size effects. These observations suggest that water under strong hydrophilic confinement may display richer phase behavior than hitherto assumed. This also suggests that propensity toward cavitation does not always correlate with greater tension, contrary to the prevailing assumption for interpreting water stretching experiments. We also show that a maximum spinodal density in water results in a locus of maximum compressibility and a minimum speed of sound that are independent from any influence of a liquid−liquid critical point (LLCP). However, we demonstrate that structural signatures of a Widom line, which likely emanates from an LLCP at elevated pressure, extend to large negative pressure, but such signatures are only observed upon sampling water's underlying potential energy landscape, rather than the thermalized metastable liquid.
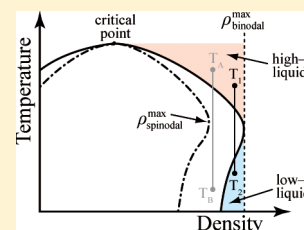
I. INTRODUCTION

Liquid water is often described as anomalous because its behavior frequently departs from that of conventional "simple" liquids. Examples of water anomalies include a temperature of maximum density (TMD) and increases in thermodynamic response functions (e.g., isothermal compressibility κ_T and isobaric heat capacity C_P[1,2]) upon isobaric cooling.[3] While departures from simple liquid behavior are certainly not unique to water, the plethora of such deviations makes this substance an extraordinary exception to the conventional rules. This has contributed to the continued interest in characterizing water's behavior across a broad range of thermodynamic conditions, including its supercooled and glassy states.[3−5]

Recently, there has been renewed interest in water's behavior at negative pressure (i.e., stretched water).[6−12] In contrast to the abundance of work on water at positive pressure, this region remains relatively unexplored. Relative to typical liquids, this region is rather vast, as the strong degree of cohesion afforded by water's hydrogen bond network allows for observed tensions up to −140 MPa.[6,13] In addition to serving as an interesting model for probing the limits of liquid cohesion, water at negative pressure is integral to vasculature in natural and engineered plants[14,15] and is also important for understanding the pressure denaturation of proteins.[16]

Part of this interest in stretched water also stems from suggestions that signatures which might distinguish between competing explanations of supercooled water's anomalies likely exist in this regime. Earlier work found evidence of a TMD at 42 °C and −140 MPa,[13] which lent credit to Speedy's conjecture that the liquid spinodal retracing to positive pressure can explain water's anomalies.[17] This is because such a scenario requires a negatively sloped TMD line in the pressure−temperature plane which is then thermodynamically required to become tangent to the liquid spinodal at its pressure minimum.[17] While thermodynamic arguments make a retracing spinodal at positive pressures problematic,[3] there is still much interest in characterizing whether the TMD increases with decreasing pressure or eventually retraces to lower temperatures.[9] Note that a retracing spinodal is possible for single component substances that contain a second, low-temperature liquid/gas critical point and a negatively sloped liquid/gas coexistence locus at low temperature, which exist in some computational models of patchy colloids.[18]

The two most frequently invoked interpretations of water anomalies in the supercooled region are the second critical point hypothesis[19] and the singularity-free scenario.[20] The former posits the existence of a liquid−liquid phase transition (LLPT) between high- and low-density liquids (HDL, LDL) that terminates at a liquid−liquid critical point (LLCP) deep in the supercooled region.[19] Water's anomalies are then consequences of being supercritical with respect to this second critical point. The singularity-free scenario shows that an increase of thermodynamic response functions upon cooling is a thermodynamic necessity for a liquid with a negatively sloped TMD in the pressure−temperature ($P−T$) plane.[20] Note that this scenario is also equivalent to the existence of an LLCP at zero absolute temperature.

Both scenarios predict a locus of extrema in thermodynamic response functions with respect to temperature along isobars,

which in the case of the second critical point hypothesis are often called Widom lines. The loci of response function extrema become arbitrarily close to each other upon approaching the critical point,[21] and hence, a common term is often used to refer to all such lines. Recent proposals[12,22] suggest that defining the Widom line as the locus along which there is a 1:1 ratio of HDL:LDL-like water molecules provides less ambiguity. We adopt this usage here (see section VI) and clarify when discussing studies where the authors refer to the locus of extrema of a thermodynamic response function as the Widom line. Computational studies routinely observe such extrema in molecular models of water.[12,21−24] However, only an increase upon isobaric cooling, without extrema, is observed experimentally.[1,2] This may be because at ambient and elevated pressures such extrema are below the temperature limit determined by homogeneous ice nucleation in a region often referred to as "no man's land." A recent study has suggested that the line of maximum compressibility emerges from no man's land at negative pressure,[7] suggesting that the doubly metastable regime (i.e., metastable to cavitation and to crystallization) may provide fresh insights into the anomalous behavior of liquid water.[8] In addition, experiments on supercooled water confined in silica nanopores, which suppresses crystal nucleation, may require reinterpretation if the recent suggestion that such water is in fact under considerable tension proves to be correct.[25]

Here, we employ molecular dynamics to study the thermodynamic behavior of water under strongly stretched conditions, produced through isochoric cooling. In section II, we revisit water's phase diagram in the temperature−density $(T−\rho)$ plane and highlight the fact that the shape of the liquid binodal and spinodal allow for isochores to exhibit "reentrant" phase behavior, whereby a system that cavitates upon isochoric cooling can then rehomogenize upon further cooling. In addition, isochores have a temperature of maximum propensity toward cavitation in the metastable region. Section III briefly describes the computational methods employed in this study. In section IV, we demonstrate that, in the TIP4P/2005 water model, isochores without a TMD can exhibit reentrant phase behavior, suggesting that greater tension along an isochore does not necessarily imply a greater propensity toward cavitation, as has been assumed in the interpretation of water stretching experiments.[6,7,13] Such behavior displays appreciable finite size effects and suggests that water may display richer phase behavior under hydrophilic confinement than previously assumed. We then show in section V that a maximum propensity toward cavitation can result in extrema in the compressibility and the speed of sound that are independent of any signatures of an LLCP emanating from elevated pressure. Finally in section VI, we show that structural signatures of an LLCP do extend to deeply negative pressure, however they are only observed upon sampling water's potential energy landscape. Section VII contains concluding remarks as well as suggestions for further study.

II. WATER'S $T−\rho$ PHASE DIAGRAM

Figure 1 contains a schematic of water's liquid/vapor phase boundaries in the temperature-density $(T−\rho)$ plane, including its metastable low-temperature extension. The feature in this plot that serves as the focal point for much of the following discussion is that the liquid binodal exhibits a maximum density $\rho_{binodal}^{max}$ (∼4 °C in real water). A $\rho_{binodal}^{max}$ in water has been known for a long time[26] and is reproduced in both theoretical descriptions[27,28] and simulations of molecular models of water.[23,29] In addition, the
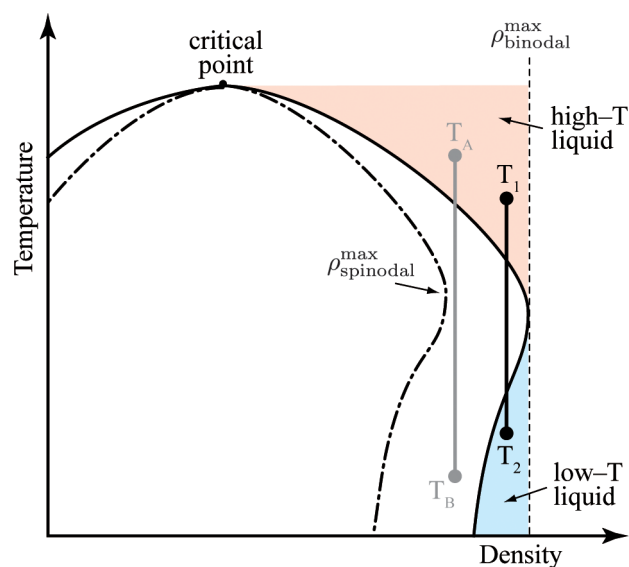

Figure 1. Schematic of water's liquid/vapor phase boundaries. Below the maximum liquid binodal density, there are two regions where the liquid is stable with respect to the vapor. Cooling isochorically to traverse from one region to another (e.g., from T_1 to T_2) can result in reentrant behavior, whereby the liquid cavitates upon cooling but then rehomogenizes upon further cooling. In both isochores, there exists a temperature in the metastable region where the liquid has a maximum propensity toward cavitation due to proximity to a $\rho_{spinodal}^{max}$, as occurs along the isochore labeled by T_A and T_B.

supercooled metastable branch of the liquid binodal and cavitation lines (the kinetic spinodal) have also recently been reported.[11]

Water with $\rho > \rho_{binodal}^{max}$ is never thermodynamically favored to cavitate. Below $\rho_{binodal}^{max}$, the equilibrium liquid can be subdivided into two portions: a high-T and a low-T region (see Figure 1). In the former, the liquid becomes metastable with respect to the vapor upon isochoric cooling; in the latter, it does so by isochoric heating. A range of isochores below $\rho_{binodal}^{max}$ can exhibit "reentrant" behavior whereby upon cooling the system would phase separate and then rehomogenize upon further cooling (assuming crystallization is avoided). In fact, homogenization upon cooling as well as cavitation upon heating have been directly observed in synthetic quartz inclusions.[11] The density range over which separate stable liquid branches exist in water is rather narrow and has been exaggerated in the figure for clarity. We stress that the low-T region, while stable with respect to cavitation, is largely metastable with respect to crystallization.

A consequence of $\rho_{binodal}^{max}$ is a maximum spinodal density $\rho_{spinodal}^{max}$, and liquid water above $\rho_{spinodal}^{max}$ is never thermodynamically unstable (as opposed to metastable) with respect to the vapor. We are not aware of any model with a $\rho_{binodal}^{max}$ in the absence of a $\rho_{spinodal}^{max}$, and numerous studies suggest that both exist for liquid water.[11,23,27,28] A $\rho_{spinodal}^{max}$ means that isochores above this density contain a point which is "closest" to the spinodal, resulting in a temperature of maximum propensity toward cavitation.

The method that has been shown to produce the highest tensions in liquid water is isochoric cooling. In order to develop tension this way, the liquid must have a positive coefficient of thermal expansion, which in the case of water, requires that temperatures not be too low. Using a microscopic Berthelot tube,[6,13] water trapped in tiny mineral inclusions develops tension as it is cooled isochorically, with tensions up to −140

MPa reported.[13] The exact pressures achieved remain uncertain because their determination often requires extrapolation of a given equation of state[30] (e.g., IAPWS-95[31]). A more accurate method employs thermodynamic integration using the speed of sound.[9]

The pioneering work of Angell and co-workers[13] on water at negative pressure in quartz inclusions noted that a particular isochore would "nucleate randomly in the range 40−47 °C and occasionally not at all." In subsequent work, Caupin and co-workers[6] studied a single isochore that exhibited a temperature with a minimum free energy barrier to cavitation T_{min}. Both cases were interpreted as the consequence of a TMD, as isochores will exhibit a minimum in pressure (i.e., largest tension) at such a point. The assumption in this case is that along an isochore, a more stretched liquid is more prone to cavitate.[6] While T_{min} does not exactly coincide with the TMD, due to the temperature variation of surface tension, the existence of T_{min} is described as being the result of a pressure minimum along an isochore.[6] In section IV, we present the results of molecular dynamics simulations of TIP4P/2005 water[32] (generally considered the most accurate classical model of water) that suggest that a larger tension in liquid water does not necessarily imply it is more prone to cavitate.

III. METHODS

Molecular dynamics simulations were performed using the GROMACS 4.6.5 simulation package.[33] For the equation of state computation (Figure 2), we simulated 4000 water molecules interacting via TIP4P/2005 potential[32] in the NVT ensemble. SETTLE[34] was used to constrain the covalent bonds in water molecules. Depending on the temperature, the simulation times varied from 10 ns to 2 μs. To compute thermodynamic response functions (Figure 3), we simulated 500 water molecules in both the NVT and NPT ensembles, and the simulation times varied between 20 ns and 4 μs.

Throughout the study, we employed a 2 fs time step. Temperature was maintained using a Nose−Hoover thermostat[35,36] with a 0.2 ps time constant, and pressure was controlled using Parrinello−Rahman barostat[37] with a 2 ps time constant. Periodic boundary conditions were applied in all three dimensions in a cubic simulation cell. The short-range interactions were truncated at 0.95 nm, and long-range dispersion corrections were applied for both pressure and energy. Long range electrostatic terms were computed by using particle mesh Ewald[38] with a grid spacing 0.12 nm.

IV. ISOCHORES OF TIP4P/2005 WATER

Figure 2 shows the pressure−temperature equation of state for isochores ranging from 0.840 to 0.920 g/cm³. Isochores with $\rho \geq$ 0.890 g/cm³ exhibit no phase transitions. In addition, a pressure minimum (i.e., a TMD), observed at ρ = 0.900 and 0.920 g/cm³, disappears at lower densities. In fact, ρ = 0.900 g/cm³ exhibits a maximum in pressure around 230 K, indicating a temperature of minimum density, a feature seen in several molecular models of water but has not been observed experimentally in bulk water.[39]

For $\rho \leq$ 0.885 g/cm³, cavitation occurs as the liquid cools, resulting in a phase-separated system. For ρ = 0.885 and 0.880 g/cm³, lowering the temperature of the two-phase system results in spontaneous homogenization to a single liquid phase, consistent with the reentrant coexistence line and spinodal shown in Figure 1. Note that these isochores do not contain a TMD, meaning that reentrant behavior is not simply the consequence of a minimum pressure. For isochores below 0.880 g/cm³, we no longer observe spontaneous homogenization upon cooling on the simulation time scales employed here. However, homogeneous systems
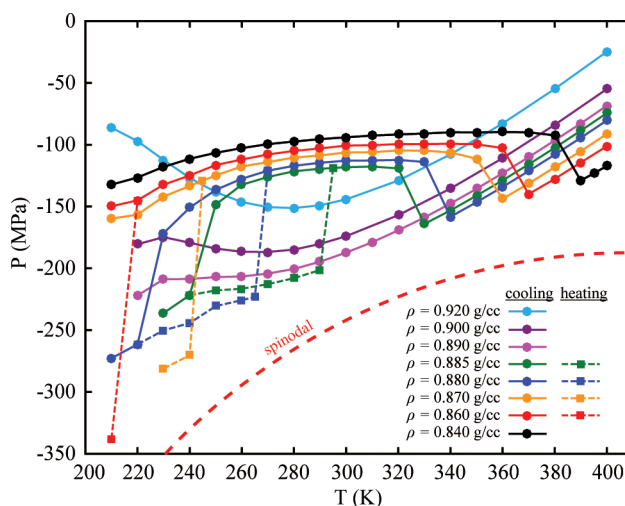

Figure 2. Equation of state for a selection of low-density isochores generated using 4000 TIP4P/2005 water molecules. Several isochores that cavitate upon cooling spontaneously homogenize upon further cooling, all of which produce liquids under greater tension than their corresponding high temperature liquid branch. Such behavior implies that reentrant behavior is not simply the consequence of a pressure minimum that accompanies a temperature of maximum density. For reference, we have included the vapor/liquid spinodal produced for ref 12. This curve has been numerically extrapolated to higher temperature from 350 K.

launched at low temperature are kinetically stable and only spontaneously cavitate upon heating.

Isochores that homogenize upon cooling exhibit hysteresis upon heating, a feature indicative of a first-order phase transition. Upon further heating of the two-phase system, we observe homogenization without any hysteresis, which is likely a result of our coarse temperature resolution and long equilibration times. However, this still suggests that the temperature range that separates the high temperature homogeneous and cavitated states (e.g., between 320 and 330 K for ρ = 0.885 g/cm³) contains a temperature where a first-order phase transition occurs.

A key observation is that isochores that rehomogenize produce a low-T liquid that is more stretched than the corresponding high-T liquid. The difference between the most stretched liquid on the high-T branch and the least stretched liquid of the low-T branch is significant: 58 MPa for ρ = 0.885 g/cm³ and 103 MPa for ρ = 0.880 g/cm³. The highest liquid tension, achieved by preparing a low-temperature homogeneous sample at ρ = 0.860 g/cm³ and T = 210 K, is −340 MPa (see Figure 2), a value more than double the limiting tensions that have been reported in the literature[6,13] and in theoretical predictions.[40] The difference between this extreme value and the tension at which this isochore initially cavitated upon cooling from much higher temperature (see Figure 2) is roughly 200 MPa.

An outstanding issue to reconcile at this point is that a bulk liquid under tension is never stable with respect to a vapor. However, we have shown that a range of low-density isochores contain two temperatures corresponding to a first order phase transition, both occurring at negative pressure. Thus, both the high and low temperature phase transitions observed along isochores (Figure 2), although originating in the reentrant behavior permitted for a range of isochores due to a $\rho_{binodal}^{max}$, cannot be strictly interpreted solely in terms of water's phase diagram (Figure 1). Evidently, the finite system size constrained to fixed volumes allows for such behavior. Since both of these

temperatures correspond to states of tension (see Figure 2), neither can correspond to equal chemical potential between liquid and vapor. Rather, they mark a point of equal Helmholtz free energy between two systems under different tensions: a homogeneous liquid and a system that contains a bubble for a collection of 4000 water molecules at the same temperature and overall density.

A likely explanation for the existence of such transitions under tension is a marked influence of interfacial effects. The thermodynamic contributions of interfaces are known to shift phase boundaries or promote new phases for small and confined systems.[41−47] The relative thermodynamic cost of forming a new interface (especially for water) is formidable for small systems. Thus, the finite system must develop significant tension before cavitation becomes thermodynamically favorable. As the thermodynamic penalty of breaking hydrogen bonds becomes more costly as water is cooled, water's interfacial tension then increases upon further cooling. Eventually, the increasing cost of maintaining an interface promotes dissolution of the bubble.

From the simulation results of TIP4P/2005 water presented above, it appears that larger tension along a given isochore does not imply a greater propensity to cavitate, which has been the common assumption in interpreting the results in water stretching experiments.[6−8,13] However, it is clear that the finite system size allows for something akin to a liquid/vapor phase transition at negative pressure that by definition do not exist in a bulk sample, since a vapor cannot exist under tension. While mineral inclusion water is typically viewed as bulk, it has been found that the homogenization temperature can depend on the size of the inclusion,[48] with smaller inclusions at the same density having lower homogenization temperatures. This observation has been rationalized through thermodynamic analyses that suggests that the size of the critical nucleus can approach that of the inclusion.[48−50] Such analyses also suggest that the influence of surface tension can result in cavitation followed by homogenization upon cooling small systems along isochores with a pressure minimum.[49] Here, we have shown that such behavior is possible for isochores without a pressure minimum, and the tension upon homogenization continues to increase upon further cooling. Therefore, it may be possible to observe greater tensions than previously assumed in sufficiently small, low-density isochores. More broadly, this work suggests that water's phase behavior under strong hydrophilic confinement may be richer than previously assumed. Specifically, it demonstrates the possibility of first-order transitions between a homogeneous liquid and liquid/bubble system at negative pressure.

V. CONSEQUENCES OF $\rho_{spinodal}^{max}$ FOR THERMODYNAMIC RESPONSE FUNCTIONS

Next, we consider the influence of a $\rho_{spinodal}^{max}$ on the behavior of thermodynamic response functions. A single component fluid's κ_T and C_P diverge at a limit of thermodynamic stability, which include spinodal curves and critical points.[51] Accordingly, isochores in the vicinity of $\rho_{spinodal}^{max}$ may exhibit maxima in thermodynamic response functions due to a minimum in proximity to a limit of stability (see example of such an isochore, labeled T_A, T_B in Figure 1). Such a locus of the extrema in thermodynamic functions would be in direct analogy to the lines of C_P^{max} and κ_T^{max} (often generically called Widom lines) that emanate from a critical point and extend into the supercritical region.

In Figure 3 we present plots of the speed of sound c, κ_T, and C_P, sampled along a selection of isochores that remain homogeneous (i.e., $\rho \geq 0.890$ g/cm^3). c is calculated through $c = \sqrt{\dfrac{C_P}{C_V}\dfrac{1}{\rho \kappa_T}}$,
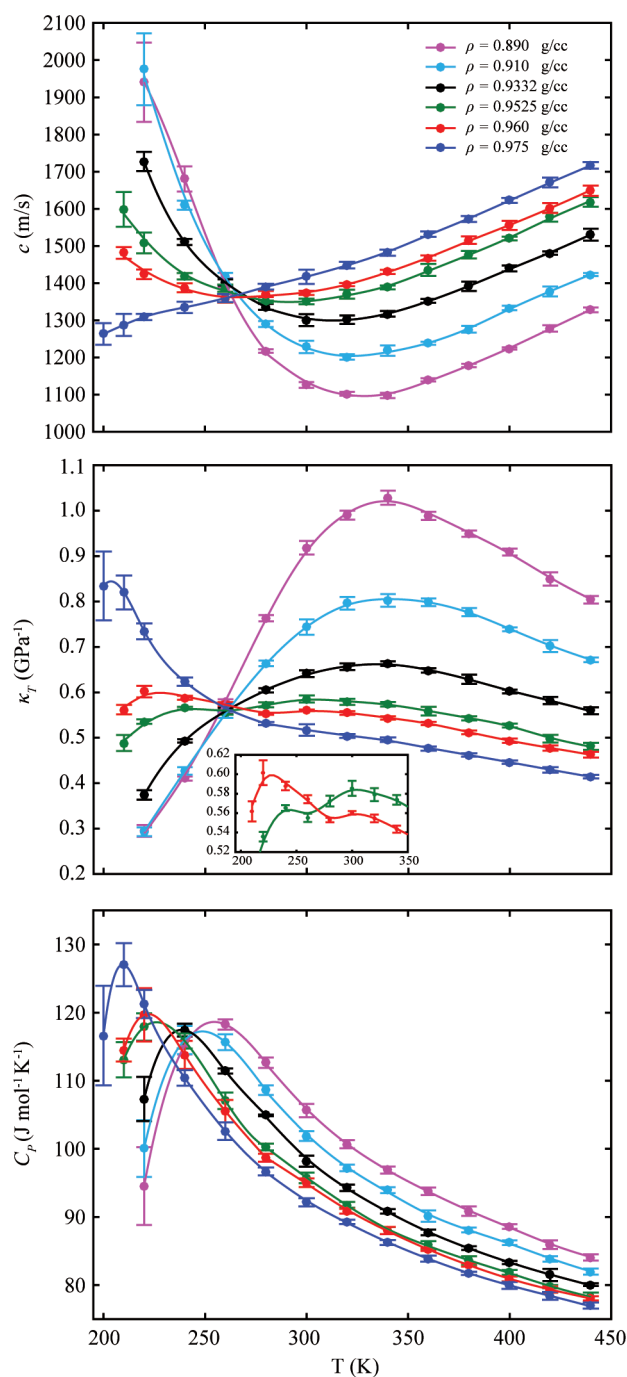

Figure 3. Isochoric temperature dependence of the speed of sound c, isothermal compressibility κ_T, and isobaric heat capacity C_P generated using 500 water molecules. c displays a minimum that weakens upon compression. For $\rho \leq 0.9332$ g/cm^3, this minimum is due to a maximum in κ_T, which itself is a result of a maximum spinodal density. Signatures of a locus of maximum κ_T emanating from higher pressure are observed at lower temperatures than spinodal-induced maxima, and $\rho = 0.9525$ and 0.960 g/cm^3 display two maxima (see inset) corresponding to these separate contributions. Such contributions are not well-separated in C_P, resulting in a nonmonotonicity in the height of the maximum upon compression. All lines are empirical guides to the eye.

where C_V is the isochoric heat capacity. C_V, C_P, and κ_T are calculated through their respective fluctuation relations

$$C_V = \frac{\langle E^2 \rangle - \langle E \rangle^2}{k_B T^2}, \quad C_P = \frac{\langle H^2 \rangle - \langle H \rangle^2}{k_B T^2},$$

$$\kappa_T = \frac{\langle V^2 \rangle - \langle V \rangle^2}{\langle V \rangle k_B T} \tag{1}$$

where E is the total energy, H is the enthalpy, V is volume, and k_B is Boltzmann's constant. C_V is calculated using the total energy under NVT conditions. Then to calculate C_P and κ_T, NPT simulations are performed using the average pressure obtained from the corresponding NVT simulation. We note here that results for two of the isochores, 0.9332 and 0.9525 g/cm³, have been previously reported.[7]

The lowest density isochore ($\rho = 0.890$ g/cm³) exhibits a strong maximum in κ_T at roughly 340 K. As density increases, the maximum steadily weakens and disappears at $\rho = 0.975$ g/cm³. We attribute $\rho_{spinodal}^{max}$ as the source of the maxima in κ_T upon cooling along isochores, as these maxima weaken upon compression. While not shown, we have also observed a spinodal-induced maximum in κ_T for the mW model.[52]

Of particular interest are the $\rho = 0.9525$ and 0.960 g/cm³ isochores, which exhibit two maxima in κ_T (see inset in Figure 3). The higher temperature maximum at roughly 320 K is clearly a point on the κ_T^{max} line emanating from the liquid spinodal. However, the lower temperature maxima around 220 K (0.960 g/cm³) and 240 K (0.9525 g/cm³) are points on the κ_T^{max} line that emanate from higher pressure.[12,22]

While we do not observe separate peaks in C_P, the strength of the maximum weakens and then increases with increasing density, suggesting that while there is no clean separation between a spinodal-induced and an LLCP-induced C_P^{max}, there is clear evidence of the effect of the spinodal. This strongly suggests that spinodal induced fluctuations affect C_P in this regime. We must note that lines of C_P^{max} and κ_T^{max} are not necessarily indicative of criticality, however in this water model there is reasonable evidence to suggest the existence of a second critical point.[12,22] In addition, secondary maxima in heat capacity have been observed in a coarse-grained lattice model of water subject to extreme confinement.[53]

Between $\rho = 0.890$ and 0.960 g/cm³, isochores display a minimum in the speed of sound, a result of either a maximum in κ_T or minimum in C_P/C_V. C_P/C_V exhibits a roughly density-independent minimum at 280 K. The minima in c for $\rho = 0.890$, 0.910, and 0.9332 g/cm³ coincide with the corresponding κ_T^{max} along these isochores and are thus a consequence of $\rho_{spinodal}^{max}$. However, the 0.9525 and 0.960 g/cm³ isochores display minima near the temperature of minimum C_P/C_V, where the influence of the liquid spinodal and a possible LLCP are interwoven.

Recent experiments of isochorically stretched water found a minimum speed of sound in the 0.9332 g/cm³ isochore.[7] The authors then performed simulations with TIP4P/2005 along this isochore and found a minimum speed of sound that is due to a compressibility maximum, a result we have reproduced in this study. The authors suggested that this point was the negative pressure extension of the κ_T^{max} locus that had previously been computed for TIP4P/2005 water.[24] They then proposed that the experiments had observed a point on the κ_T^{max} locus, which had previously eluded observation on account of rapid crystallization, and which "emerges from the no man's land at negative pressure".[7] Our extensive computational investigation suggests

that, depending on the particular isochore under investigation, this high temperature minimum in the speed of sound can originate either from a κ_T^{max} or a minimum in C_P/C_V. However, κ_T^{max} is not the negative pressure extension of a line emanating from higher pressure. Instead, it is due to the peculiar behavior of water's spinodal in its $T-\rho$ phase diagram and originates at negative pressure. We stress that this assessment is limited to the behavior of TIP4P/2005 water and that the origin of the minimum c in the experiments remains to be clarified. If one were to observe that the minimum speed of sound intensifies upon decompression from 0.9332 g/cm³ and disappears upon compression, similar to the behavior seen in Figure 3 (top), then it is likely that such minima in c are spinodal-induced.

Thus, one can include an additional line of κ_T^{max} to TIP4P/2005's phase diagram of anomalies in the $P - T$ plane (Figure 4).
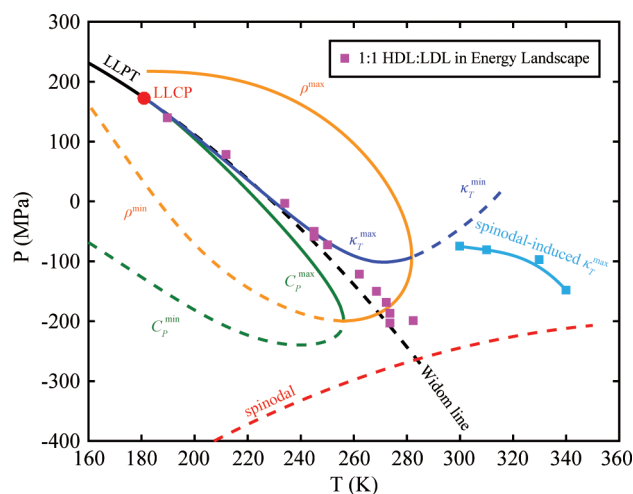

Figure 4. Phase diagram of anomalies in TIP4P/2005 water. A maximum spinodal density results in a locus of compressibility maxima that is well-separated from the κ_T^{max} originating at high pressure. However, the spinodal-induced κ_T^{max} is only observed through isochoric sampling, which is the typical pathway for experiments of stretched water. The locus of equal proportions of HDL and LDL water molecules in water's potential energy landscape follows the Widom line well into the negative pressure regime and suggests that a crossover from HDL to LDL dominance in the structure of water could be observed at higher temperatures than the C_P^{max} in highly stretched water. All curves aside from the spinodal-induced κ_T^{max} and 1:1 HDL:LDL in the potential energy landscape are two-structure equation of state fits originally published in ref 12.

However, this additional κ_T^{max} line is limited to isochoric paths, the relevant pathway for experiments achieving such high tensions. This line is well separated from the previously calculated κ_T^{max} line that is suspected to emanate from an LLCP[12,23] (shown in Figure 4). While an LLCP-induced κ_T^{max} does not extend below −100 MPa, we have found that signatures of an LLCP, observed by sampling water's potential energy landscape, extend much deeper into water's stretched regime as well as higher temperatures.

VI. STRUCTURAL SIGNATURES OF A WIDOM LINE IN THE POTENTIAL ENERGY LANDSCAPE

We now present a structural analysis that demonstrates how signatures of the Widom line, which can be interpreted as the analytical extension of the liquid−liquid coexistence line,[22] extend to extreme negative pressures. Specifically, we consider

the structure of water's potential energy landscape. Sampling a system's potential energy landscape by producing a representative ensemble of potential energy minima (i.e., inherent structures) can clarify structural features that are otherwise obscured by thermal fluctuations.[54,55] A liquid's inherent structures correspond physically to the "glass" produced through an infinitely rapid isochoric quench to $T = 0$ K.

Recent studies have shown that water's inherent structures display a bimodal distribution of local structure index (LSI), a local structural order parameter that quantifies the degree of separation between the first and second hydration shells, in both SPC/E[56,57] and TIP4P/2005.[58] LSI for a given water molecule i is defined by

$$\text{LSI}(i) = \frac{1}{n(i)} \sum_{j=1}^{n(i)} [\Delta(j;\, i) - \bar{\Delta}(i)]^2 \qquad (2)$$

where $\Delta(j;i) = r_{j+1} - r_j$ [i.e., the oxygen−oxygen distance of the jth nearest neighbor subtracted from the $(j + 1)$th] and $\bar{\Delta}(i)$ is the average over the $n(i)$ nearest neighbors defined to be within a cutoff of 3.7 Å.[59] Weak bimodality in the equilibrated liquid is observed only at extreme supercooling. A smaller LSI value implies a more disordered, HDL-like environment, and a larger LSI value corresponds to a more ordered, LDL-like environment. Thus, generating inherent structures appears to clarify the underlying structural features corresponding to these two distinct local environments.

It was shown that, in TIP4P/2005 water, the Widom line, defined in this case as the $\kappa_T^{\max}$ line generated along isobars, closely corresponds to a 1:1 distribution of HDL:LDL in the inherent structures for pressures from 1 to 1500 bar.[58] Note that in this pressure range, the lines of $C_P^{\max}$, $\kappa_T^{\max}$, and the Widom line differ by at most 10 K, so they are often collectively called the Widom line. As pressure decreases, these lines grow further apart, and only the Widom line is expected to intersect the spinodal in the deeply stretched region (see Figure 4).

Through steepest descent potential energy minimization, we have generated the inherent structures along isochores that avoid cavitation (i.e., $\rho > 0.885$ g/cm^3) and calculated their LSI. In agreement with previous observations,[58] we observe a bimodal LSI distribution with a minimum around 0.13, a value that is independent of the thermodynamic conditions. In Figure 5, we have provided an example of the LSI distributions sampled along the 0.890 g/cm^3 isochore. Using 0.13 as the cutoff to distinguish a water molecule as either HDL or LDL-like, we estimate the temperature of 1:1 HDL:LDL ratio along an isochore by mapping the equilibrated liquid onto the underlying potential energy landscape and performing the LSI calculation on the resulting inherent structures. We then find the corresponding pressure of the equilibrated liquid from its equation of state. Here, we have extended the line of 1:1 HDL:LDL in the $P-T$ plane from elevated pressure well into the negative pressure regime (Figure 4).

In agreement with earlier work,[58] we observe that the 1:1 HDL:LDL line follows the line of $\kappa_T^{\max}$ at positive pressure. At negative pressure, this trend breaks down, as the locus of 1:1 HDL:LDL in inherent structures appears to roughly follow the Widom line predicted by two-structure equation of state fitting.[12] If this were to be the case for real water, this would suggest that signatures of an LLCP would be accessible in the deeply stretched region at higher temperature than $C_P^{\max}$. Molecular simulations have found that the HDL:LDL ratio estimated from the inherent structures is in the neighborhood of estimates from
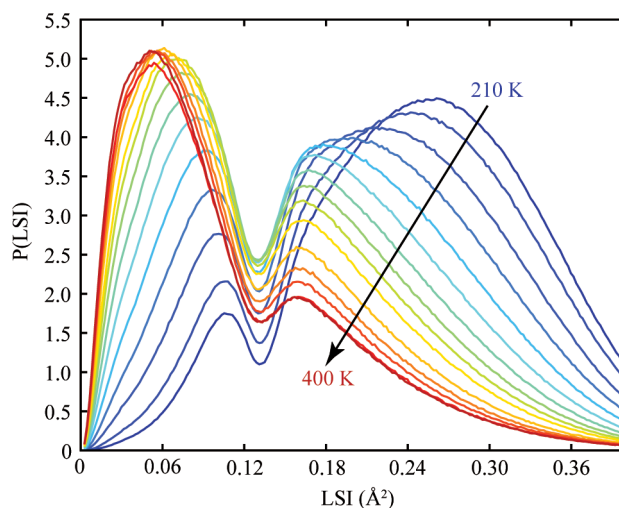

Figure 5. Local structure index (LSI) distribution for inherent structures along the 0.890 g/cm^3 isochore. At low temperature, the dominant local environment is a more ordered, LDL-like structure (i.e., larger LSI), and at higher temperature a more disordered, HDL-like local structure (i.e., smaller LSI) prevails. All peaks are separated by a minimum at roughly 0.13, providing a convenient cutoff to differentiate HDL- and LDL-like water molecules.

X-ray adsorption[60] and emission[61] of liquid water at ambient conditions.[58] While HDL is the predominant local structure at elevated temperatures, the LDL fraction grows upon cooling. The present work suggests that a crossover from HDL to LDL dominance may be observed in liquid water at extreme negative pressures.

VII. CONCLUSIONS

One way in which water deviates from conventional liquids is in the fact that the liquid binodal has a maximum density, allowing in principle for isochores to exhibit homogenization upon cooling. In finite isochoric systems, an analogous transition occurs in the absence of a TMD. However, since such transitions occur at negative pressure, they are more faithfully interpreted as a homogeneous to cavitated transition rather than a liquid to vapor transition. It is expected that such transitions can be realized in sufficiently small mineral inclusions.[49,50] In addition, this work suggests that much smaller inclusions may be a route to producing liquid water under much greater tension than theory[40] and experiment[6,13] have so far suggested to be possible. Whether small enough isochoric systems are experimentally feasible remains to be clarified.

A maximum spinodal density gives rise to a line of $\kappa_T^{\max}$ that is independent of any Widom line emanating from higher pressure, with the latter associated with an LLCP. While signatures of a possible LLCP-induced $\kappa_T^{\max}$ line have been observed in the TIP4P/2005 model,[12,22−24] they exist at significantly lower temperature and extend to −100 MPa. However, we have shown that structural signatures of a Widom line extending to much larger negative pressures lie hidden in water's energy landscape. If the Widom line in real water crosses the homogeneous nucleation line at negative pressure, it is unlikely to emerge as a locus of extrema in thermodynamic response functions. Rather one would seek to observe a locus of 1:1 HDL:LDL-like water molecules, which may be possible with existing experimental techniques.[60,61]

Much of what we have discussed here, specifically reentrant behavior and spinodal-induced extrema in thermodynamic response functions, is relevant to any liquid that contains a $\rho_{\mathrm{binodal}}^{\max}$, which should exist in liquids with density anomalies. This includes other tetrahedrally coordinated liquids (e.g., silicon and germanium) as well as the numerous patchy colloidal models. Some patchy colloids have also been shown to have a minimum "vapor" binodal density[18] which should also result in lines of extrema of thermodynamic response functions.

■ AUTHOR INFORMATION

Corresponding Author

*E-mail: pdebene@princeton.edu.

ORCID ◉

Pablo G. Debenedetti: 0000-0003-1881-1728

Author Contributions

§Y.E.A. and R.S.S. contributed equally to this work.

Notes

The authors declare no competing financial interest.

■ REFERENCES

(1) Angell, C. A.; Shuppert, J.; Tucker, J. C. Anomalous properties of supercooled water. Heat capacity, expansivity, and proton magnetic resonance chemical shift from 0 to −38. *J. Phys. Chem.* **1973**, *77* (26), 3092−3099.

(2) Speedy, R. J.; Angell, C. A. Isothermal compressibility of supercooled water and evidence for a thermodynamic singularity at −45°C. *J. Chem. Phys.* **1976**, *65* (3), 851−858.

(3) Debenedetti, P. G. Supercooled and Glassy Water. *J. Phys.: Condens. Matter* **2003**, *15* (45), R1669−R1726.

(4) Gallo, P.; Amann-Winkel, K.; Angell, C. A.; Anisimov, M. A.; Caupin, F.; Chakravarty, C.; Lascaris, E.; Loerting, T.; Panagiotopoulos, A. Z.; Russo, J.; Sellberg, J. A.; Stanley, H. E.; Tanaka, H.; Vega, C.; Xu, L. M.; Pettersson, L. G. M. Water: A Tale of Two Liquids. *Chem. Rev.* **2016**, *116* (13), 7463−7500.

(5) Nilsson, A.; Pettersson, L. G. M. The structural origin of anomalous properties of liquid water. *Nat. Commun.* **2015**, *6*, 8998.

(6) Azouzi, M. E.; Ramboz, C.; Lenain, J. F.; Caupin, F. A coherent picture of water at extreme negative pressure. *Nat. Phys.* **2013**, *9* (1), 38−41.

(7) Pallares, G.; Azouzi, M. E.; Gonzalez, M. A.; Aragones, J. L.; Abascal, J. L. F.; Valeriani, C.; Caupin, F. Anomalies in bulk supercooled water at negative pressure. *Proc. Natl. Acad. Sci. U. S. A.* **2014**, *111* (22), 7936−7941.

(8) Caupin, F. Escaping the no man's land: Recent experiments on metastable liquid water. *J. Non-Cryst. Solids* **2015**, *407*, 441−448.

(9) Pallares, G.; Gonzalez, M. A.; Abascal, J. L. F.; Valeriani, C.; Caupin, F. Equation of state for water and its line of density maxima down to −120 MPa. *Phys. Chem. Chem. Phys.* **2016**, *18* (8), 5896−5900.

(10) Menzl, G.; Gonzalez, M. A.; Geiger, P.; Caupin, F.; Abascal, J. L. F.; Valeriani, C.; Dellago, C. Molecular mechanism for cavitation in water under tension. *Proc. Natl. Acad. Sci. U. S. A.* **2016**, *113* (48), 13582−13587.

(11) Qiu, C.; Kruger, Y.; Wilke, M.; Marti, D.; Ricka, J.; Frenz, M. Exploration of the phase diagram of liquid water in the low-temperature metastable region using synthetic fluid inclusions. *Phys. Chem. Chem. Phys.* **2016**, *18* (40), 28227−28241.

(12) Biddle, J. W.; Singh, R. S.; Sparano, E. M.; Ricci, F.; Gonzalez, M. A.; Valeriani, C.; Abascal, J. L. F.; Debenedetti, P. G.; Anisimov, M. A.; Caupin, F. Two-structure thermodynamics for the TIP4P/2005 model of water covering supercooled and deeply stretched regions. *J. Chem. Phys.* **2017**, *146* (3), 034502.

(13) Zheng, Q.; Durben, D. J.; Wolf, G. H.; Angell, C. A. Liquids at Large Negative Pressure: Water at the Homogeneous Nucleation Limit. *Science* **1991**, *254* (5033), 829−832.

(14) Wheeler, T. D.; Stroock, A. D. The transpiration of water at negative pressures in a synthetic tree. *Nature* **2008**, *455* (7210), 208−212.

(15) Stroock, A. D.; Pagay, V. V.; Zwieniecki, M. A.; Holbrook, N. M. The Physicochemical Hydrodynamics of Vascular Plants. In *Annual Review of Fluid Mechanics*; Davis, S. H., Moin, P., Eds.; Annual Reviews: Palo Alto, 2014; Vol. 46, pp 615−642.

(16) Bianco, V.; Franzese, G. Contribution of Water to Pressure and Cold Denaturation of Proteins. *Phys. Rev. Lett.* **2015**, *115* (10), 108101.

(17) Speedy, R. J. Stability-limit conjecture. An interpretation of the properties of water. *J. Phys. Chem.* **1982**, *86* (6), 982−991.

(18) Rovigatti, L.; Bianco, V.; Tavares, J. M.; Sciortino, F. Communication: Re-entrant limits of stability of the liquid phase and the Speedy scenario in colloidal model systems. *J. Chem. Phys.* **2017**, *146* (4), 041103.

(19) Poole, P. H.; Sciortino, F.; Essmann, U.; Stanley, H. E. Phase behaviour of metastable water. *Nature* **1992**, *360* (6402), 324−328.

(20) Sastry, S.; Debenedetti, P. G.; Sciortino, F.; Stanley, H. E. Singularity-free interpretation of the thermodynamics of supercooled water. *Phys. Rev. E: Stat. Phys., Plasmas, Fluids, Relat. Interdiscip. Top.* **1996**, *53* (6), 6144−6154.

(21) Xu, L. M.; Kumar, P.; Buldyrev, S. V.; Chen, S. H.; Poole, P. H.; Sciortino, F.; Stanley, H. E. Relation between the Widom line and the dynamic crossover in systems with a liquid-liquid phase transition. *Proc. Natl. Acad. Sci. U. S. A.* **2005**, *102* (46), 16558−16562.

(22) Singh, R. S.; Biddle, J. W.; Debenedetti, P. G.; Anisimov, M. A. Two-state thermodynamics and the possibility of a liquid-liquid phase transition in supercooled TIP4P/2005 water. *J. Chem. Phys.* **2016**, *144* (14), 144504.

(23) Gonzalez, M. A.; Valeriani, C.; Caupin, F.; Abascal, J. L. F. A comprehensive scenario of the thermodynamic anomalies of water using the TIP4P/2005 model. *J. Chem. Phys.* **2016**, *145* (5), 054505.

(24) Abascal, J. L. F.; Vega, C. Widom line and the liquid-liquid critical point for the TIP4P/2005 water model. *J. Chem. Phys.* **2010**, *133* (23), 234502.

(25) Soper, A. K. Radical re-appraisal of water structure in hydrophilic confinement. *Chem. Phys. Lett.* **2013**, *590*, 1−15.

(26) Osborne, N. S.; Stimson, H. F.; Ginnings, D. C. Thermal properties of saturated water and steam. *Journal of Research of the National Bureau of Standards* **1939**, *23*, 261−270.

(27) Poole, P. H.; Sciortino, F.; Grande, T.; Stanley, H. E.; Angell, C. A. Effect of hydrogen bonds on the thermodynamic behavior of liquid water. *Phys. Rev. Lett.* **1994**, *73* (12), 1632−1635.

(28) Truskett, T. M.; Debenedetti, P. G.; Sastry, S.; Torquato, S. A single-bond approach to orientation-dependent interactions and its implications for liquid water. *J. Chem. Phys.* **1999**, *111* (6), 2647−2656.

(29) Brovchenko, I.; Geiger, A.; Oleinikova, A. Liquid-liquid phase transitions in supercooled water studied by computer simulations of various water models. *J. Chem. Phys.* **2005**, *123* (4), 044515.

(30) Holten, V.; Sengers, J. V.; Anisimov, M. A. Equation of State for Supercooled Water at Pressures up to 400 MPa. *J. Phys. Chem. Ref. Data* **2014**, *43* (4), 043101.

(31) Wagner, W.; Pruss, A. The IAPWS formulation 1995 for the thermodynamic properties of ordinary water substance for general and scientific use. *J. Phys. Chem. Ref. Data* **2002**, *31* (2), 387−535.

(32) Abascal, J. L. F.; Vega, C. A general purpose model for the condensed phases of water: TIP4P/2005. *J. Chem. Phys.* **2005**, *123* (23), 234505.

(33) Van der Spoel, D.; Lindahl, E.; Hess, B.; Groenhof, G.; Mark, A. E.; Berendsen, H. J. C. GROMACS: Fast, flexible, and free. *J. Comput. Chem.* **2005**, *26* (16), 1701−1718.

(34) Miyamoto, S.; Kollman, P. A. An analytical version of the SHAKE and RATTLE algorithm for rigid water models, SETTLE. *J. Comput. Chem.* **1992**, *13* (8), 952−962.

(35) Hoover, W. G. Canonical dynamics: Equilibrium phase-space distributions. *Phys. Rev. A: At., Mol., Opt. Phys.* **1985**, *31* (3), 1695−1697.

(36) Nosé, S. A unified formulation of the constant temperature molecular dynamics methods. *J. Chem. Phys.* **1984**, *81* (1), 511−519.

(37) Parrinello, M.; Rahman, A. Polymorphic transitions in single crystals: A new molecular dynamics method. *J. Appl. Phys.* **1981**, *52* (12), 7182−7190.

(38) Essmann, U.; Perera, L.; Berkowitz, M. L.; Darden, T.; Lee, H.; Pedersen, L. G. A smooth particle mesh Ewald method. *J. Chem. Phys.* **1995**, *103* (19), 8577−8593.

(39) Liu, D. Z.; Zhang, Y.; Chen, C. C.; Mou, C. Y.; Poole, P. H.; Chen, S. H. Observation of the density minimum in deeply supercooled confined water. *Proc. Natl. Acad. Sci. U. S. A.* **2007**, *104* (23), 9570−9574.

(40) Blander, M.; Katz, J. L. Bubble nucleation in liquids. *AIChE J.* **1975**, *21* (5), 833−848.

(41) MacDowell, L. G.; Virnau, P.; Muller, M.; Binder, K. The evaporation/condensation transition of liquid droplets. *J. Chem. Phys.* **2004**, *120* (11), 5293.

(42) Rasaiah, J. C.; Garde, S.; Hummer, G. Water in Nonpolar Confinement: From Nanotubes to Proteins and Beyond. *Annu. Rev. Phys. Chem.* **2008**, *59*, 713−740.

(43) Schrader, M.; Virnau, P.; Binder, K. Simulation of vapor-liquid coexistence in finite volumes: A method to compute the surface free energy of droplets. *Phys. Rev. E* **2009**, *79* (6), 061104.

(44) Binder, K.; Block, B. J.; Virnau, P.; Troster, A. Beyond the Van Der Waals loop: What can be learned from simulating Lennard-Jones fluids inside the region of phase coexistence. *Am. J. Phys.* **2012**, *80* (12), 1099.

(45) Altabet, Y. E.; Debenedetti, P. G. The role of material flexibility on the drying transition of water between hydrophobic objects: A thermodynamic analysis. *J. Chem. Phys.* **2014**, *141* (18), 18C531.

(46) Altabet, Y. E.; Haji-Akbari, A.; Debenedetti, P. G. Effect of material flexibility on the thermodynamics and kinetics of hydrophobically induced evaporation of water. *Proc. Natl. Acad. Sci. U. S. A.* **2017**, *114* (13), E2548−E2555.

(47) MacDowell, L. G.; Shen, V. K.; Errington, J. R. Nucleation and cavitation of spherical, cylindrical, and slablike droplets and bubbles in small systems. *J. Chem. Phys.* **2006**, *125* (3), 034705.

(48) Fall, A.; Rimstidt, J. D.; Bodnar, R. J. The effect of fluid inclusion size on determination of homogenization temperature and density of liquid-rich aqueous inclusions. *Am. Mineral.* **2009**, *94* (11−12), 1569−1579.

(49) Marti, D.; Kruger, Y.; Fleitmann, D.; Frenz, M.; Ricka, J. The effect of surface tension on liquid-gas equilibria in isochoric systems and its application to fluid inclusions. *Fluid Phase Equilib.* **2012**, *314*, 13−21.

(50) Wilhelmsen, O.; Bedeaux, D.; Kjelstrup, S.; Reguera, D. Communication: Superstabilization of fluids in nanocontainers. *J. Chem. Phys.* **2014**, *141* (7), 071103.

(51) Debenedetti, P. G. *Metastable Liquids: Concepts and Principles*; Princeton University Press: Princeton, 1996.

(52) Molinero, V.; Moore, E. B. Water Modeled As an Intermediate Element between Carbon and Silicon. *J. Phys. Chem. B* **2009**, *113* (13), 4008−4016.

(53) Mazza, M. G.; Stokely, K.; Stanley, H. E.; Franzese, G. Effect of pressure on the anomalous response functions of a confined water monolayer at low temperature. *J. Chem. Phys.* **2012**, *137* (20), 204502.

(54) Stillinger, F. H.; Weber, T. A. Hidden structure in liquids. *Phys. Rev. A: At., Mol., Opt. Phys.* **1982**, *25* (2), 978.

(55) Stillinger, F. H.; Weber, T. A. Packing structures and transitions in liquids and solids. *Science* **1984**, *225* (4666), 983.

(56) Appignanesi, G. A.; Fris, J. A. R.; Sciortino, F. Evidence of a two-state picture for supercooled water and its connections with glassy dynamics. *Eur. Phys. J. E: Soft Matter Biol. Phys.* **2009**, *29* (3), 305−310.

(57) Accordino, S. R.; Fris, J. A. R.; Sciortino, F.; Appignanesi, G. A. Quantitative investigation of the two-state picture for water in the normal liquid and the supercooled regime. *Eur. Phys. J. E: Soft Matter Biol. Phys.* **2011**, *34* (5), 7.

(58) Wikfeldt, K. T.; Nilsson, A.; Pettersson, L. G. M. Spatially inhomogeneous bimodal inherent structure of simulated liquid water. *Phys. Chem. Chem. Phys.* **2011**, *13* (44), 19918−19924.

(59) Shiratani, E.; Sasai, M. Molecular scale precursor of the liquid-liquid phase transition of water. *J. Chem. Phys.* **1998**, *108* (8), 3264−3276.

(60) Wernet, P.; Nordlund, D.; Bergmann, U.; Cavalleri, M.; Odelius, M.; Ogasawara, H.; Naslund, L. A.; Hirsch, T. K.; Ojamae, L.; Glatzel, P.; Pettersson, L. G. M.; Nilsson, A. The structure of the first coordination shell in liquid water. *Science* **2004**, *304* (5673), 995−999.

(61) Tokushima, T.; Harada, Y.; Takahashi, O.; Senba, Y.; Ohashi, H.; Pettersson, L. G. M.; Nilsson, A.; Shin, S. High resolution X-ray emission spectroscopy of liquid water: The observation of two structural motifs. *Chem. Phys. Lett.* **2008**, *460* (4−6), 387−400.